Comparison of Two Alternative Hydraulic PTO Concepts for Wave Energy Conversion

Ronan Costello[#1], John V. Ringwood[#2] and Jochem Weber[*3]

[#]*Centre for Ocean Energy Research, National University of Ireland, Maynooth, Ireland.*

[1]ronan.costello@eeng.nuim.ie

[2]john.ringwood@eeng.nuim.ie

[*]*Wavebob Ltd. Ireland.*

[3]jochem.weber@wavebob.com

***Abstract*— Hydraulic Power Take Off (PTO) systems for wave energy usually fall into two broad categories. These are, firstly, variable pressure systems where control of the primary force/torque is achieved by pressure modulation, and secondly, constant pressure systems where control of the primary force/torque is achieved by valve transitions that select between discrete effort levels determined by the approximately constant accumulator pressure and alternative piston areas. Energy storage is integral to the constant pressure category while, in the purest form of the variable pressure category, it is not provided. Hybrid systems which combine elements of both categories are also possible.**

This paper reports an analysis of the most elementary of systems from each of these categories. The analysis uses a coupled hydrodynamic-hydraulic time domain model. The model is used to assess the effectiveness of the hydrodynamic power absorption and the efficiency of the hydraulic power transmission.

The results show that, in each case, the hydraulic motor performance is a critical consideration and the optimal configuration of any one system is dependent on motor selection. In the best instances of both categories of PTO, the indicated performance is sufficiently high to facilitate commercial viability of such systems.

***Keywords*— power take off, hydraulics for wave energy, hydrostatic power transmission, variable pressure system, constant pressure system, energy storage, high efficiency, electro-hydraulic control.**

I. INTRODUCTION

To date, of the research that has been published on analysis of Wave Energy Converter (WEC) hydraulic PTO performance, the majority has focused on assessing the impact of system design on the nature and controllability of the primary force and the implications of this for power absorption, [1]-[5].

Work to date that has addressed the power flows, including losses, within a hydraulic PTO system with a view to quantifying the average rate at which energy is exported from the device rather than the rate at which it is imported from the ocean includes that by Henderson [6] Payne [7] and Plummer [8]. Henderson presents the performance of a commercially developed PTO for the Pelamis device, the system is optimised and the reported efficiencies are high. The analysis of Payne focuses on the Digital Displacement® motor technology, the mechanisms that give its performance advantages over conventional axial piston motors and its possible application to the Pelamis device. The performance of a hydraulic PTO featuring a hydraulic transformer is quantified by Plummer for a heaving vertical cylinder in a panchromatic sea. The system analysed features series power flow through multiple hydraulic machines and consequently the reported efficiency of that system is low.

The motivation for this paper is to present an analysis of the most elementary systems in each of the categories introduced above (constant pressure and variable pressure) in an effort to identify the strengths and weaknesses of each so that, where appropriate, further development of more sophisticated systems with superior performance is motivated and informed by the weaknesses exposed by analysis.

II. VARIABLE PRESSURE PTO SYSTEM.

Figure 1 shows a variable pressure PTO system in what is close to its least complicated form. The system comprises a single cylinder coupled hydraulically to a single variable displacement motor which, in turn, is coupled to a rotating electrical generator. The generator may be fixed or variable speed. In this type of system the cylinder ports are connected directly to the motor ports, there are no valves in the main flow lines. The force is controlled by controlling the pressure difference between the two lines; depending on the force actuated by the system either line A or line B may be the more highly pressurised. The motor, therefore, is required to provide four quadrant operation, i.e. the capability to accept or deliver fluid power with fluid flow in either direction. In the case where a motor cannot provide four quadrant operation, equivalent functionality is possible with the addition of appropriate directional control valves.

Further equipment shown includes a relief valve to protect the system from over pressure and an accumulator which prevents cavitation in the low pressure side of the cylinder. The check valves shown select the highest pressure of lines A & B to connect to the relief valve inlet and the lowest pressure line to connect to the low pressure accumulator. Flow resistances are indicated on the main flow lines, these represent an unavoidable energy loss due to the energy expended in pumping the working fluid through the system.

The maximum force, F_{max}, neglecting flow losses and seal friction, is

$$F_{\max} = \Delta P_{rv} A_{cyl} \tag{1}$$

where ΔP_{rv} is the relief valve set pressure and A_{cyl} is the effective piston area.

The limiting velocity, v_{lim}, neglecting compression and leakage flows, is

$$v_{\lim} = \frac{Q_{\max}}{A_{cyl}} \quad (2)$$

where Q_{max} is the maximum flow capacity of the motor.

At velocities in the range $[-v_{lim},v_{lim}]$ the force is arbitrarily controllable in the range $[-F_{max},F_{max}]$, this allows complex conjugate control or any other control approach.

Velocities outside this range are possible but, at such velocities, the flow generated by the cylinder will be in excess of the maximum flow capacity of the motor and some flow will pass through the relief valve. It follows that, at all such velocities; the cylinder differential pressure is fixed at the relief valve set pressure which sets the force to its maximum magnitude.

The parameters of the system hardware that must be chosen by the designer for the most basic analysis are:

- A_{cyl}, the effective area of the cylinder,
- D, the displacement of the motor,
- ΔP_{rv}, the relief valve set pressure,
- χ, a pipe sizing design parameter, and
- ω, the shaft speed, (or ω_{max} if variable speed).

χ is more fully defined in section C below.

An electronic controller for the system would have the displacement fraction of the motor as its principal manipulated variable and the force actuated by the cylinder as its controlled variable. In the case of a variable speed system the additional manipulated and controlled variables are, respectively, generator torque and shaft speed.

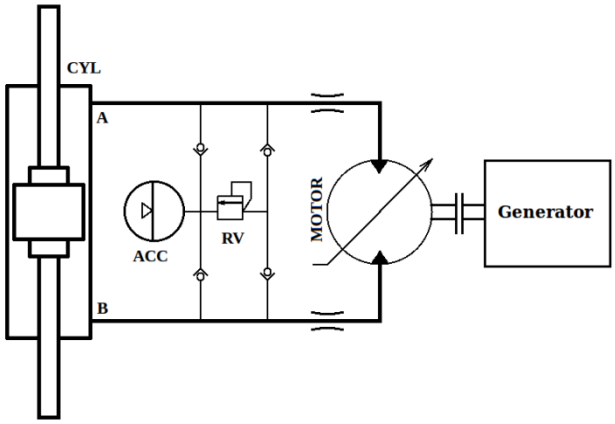

Figure 1 A variable pressure PTO system. Comprising; cylinder, motor, generator, low pressure accumulator, relief valve and check valves. Essential auxiliaries not shown include a charge pump as well as cooling and filtration systems.

III. CONSTANT PRESSURE PTO SYSTEM

Figure 2 shows the alternative to the variable pressure concept, a constant pressure PTO. Consistent with the motivations of this paper, and similarly to the system shown in Figure 2, the system shown is close to the minimum complexity embodiment of this category of PTO. The system shown is similar to that analysed by [3] and can be viewed as a simplified, single cylinder, version of that reported by [6].

The system comprises a low pressure accumulator, a high pressure accumulator, a cylinder which pumps net fluid flow from low to high pressure accumulators and a motor which controls fluid flow from high to low pressure accumulators and drives a rotating generator. Like the previous system the generator may be fixed or variable speed. Unlike the previous system the flow through the circuit is generally unidirectional, rather than reversing, and, as a consequence, four-quadrant operation is not required of the motor but valves are required to commutate, or otherwise control, the reversing flows generated by the cylinder.

A three position directional valve is included in the circuit of Figure 2. The middle position is an idle or declutched mode, it connects the ports of the cylinder to each other and to low pressure, in this mode the flow between the cylinder and the high pressure accumulator is zero and the PTO force developed by the cylinder is only that due to parasitic pressure differentials and seal friction. In the other positions one cylinder port is connected to high pressure and the other to low pressure, a high PTO force is developed and flows are generated between the cylinder and the accumulators. No particular valve technology is implicitly indicated by the symbol used. It is worth noting that the valve need not be a spool valve and, at the flowrates required in wave energy, is more likely to be assembled from a number of piloted cartridge valves.

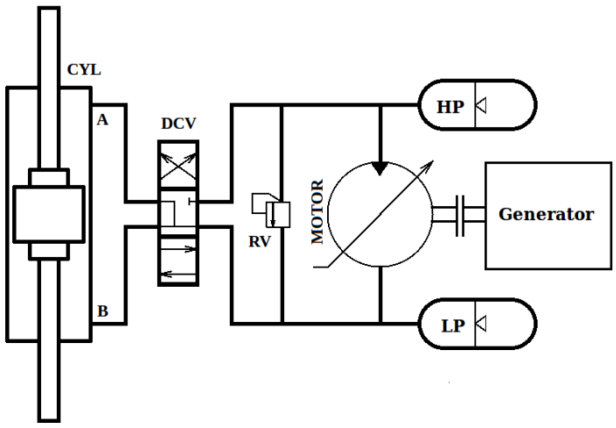

Figure 2 A constant pressure PTO system. Comprising; cylinder, directional control valve, high and low pressure accumulators, motor, generator, and relief valve. Essential auxiliaries not shown include a charge pump as well as cooling and filtration systems.

The most straightforward control of the valve would be rectification i.e. to always connect the contracting chamber of the cylinder to the high pressure accumulator and the expanding chamber to the low pressure accumulator and, so, never use the middle position of the valve. A more advanced control would, in an effort to promote resonance and increase energy absorption from the ocean, mix in periods of idling, as in [3] or of reverse flow, as in [9].

The parameters of the system hardware that must be chosen by the designer for the most basic analysis, which assumes constant pressure accumulators, are in fact identical to those listed in the preceding section for the variable pressure PTO.

An electronic controller for this system has the PTO force and motor flowrate as the controlled variables and the valve state and motor displacement as the respective manipulated variables. In the case of a variable speed system the additional manipulated and controlled variables are, respectively, generator torque and shaft speed.

IV. Model of System Components

The following sections present the equations used to model the principal components that are common to both the variable pressure and constant pressure PTO systems.

A. Motor Performance

The flow and torque performance of rotating hydraulic machines is described by [10]. The general structure of the equations (3) to (12) is valid for a broad range of machinery. With appropriate selection of the coefficients, the performance of axial piston, radial piston and gear types can be accurately evaluated. The sign convention used is that normally seen for a pump [10] but the formulation of the loss terms is robust enough to cover all modes of operation. All permutations of sign in shaft speed, applied differential pressure and displacement fraction are valid and hence power flow may be either from fluid to shaft or vice versa. This flexibility is particularly necessary if idle losses and reverse power flow in the PTO are to be modelled correctly.

The ideal volumetric flow through a pump or motor, q_i, and the ideal shaft torque developed, t_i, are:

$$q_i = xD\varpi \tag{3}$$

$$t_i = xD\Delta p \tag{4}$$

Where ω is the motor shaft speed, D is its cubic displacement per unit shaft rotation and Δp is the pressure differential applied across the motor ports. x is the motor displacement fraction, which may, in the most versatile variable displacement designs, take any value in the range [-1,1] or, in less versatile designs, in the range [0,1] (or say [0.2,1]). In fixed displacement designs x=1. The real flow and torque are calculated by adjusting the ideal values for the flow loss, q_{loss}, and the torque loss, t_{loss};

$$q_r = q_i - q_{loss} \tag{5}$$

$$t_r = t_i + t_{loss} \tag{6}$$

The flow and torque losses are:

$$q_{loss} = q^*_{loss} D\varpi_{\max} \operatorname{sign}(\Delta p) \tag{7}$$

$$t_{loss} = t^*_{loss} D\Delta p_{\max} \operatorname{sign}(\varpi) \tag{8}$$

Where q^*_{loss} and t^*_{loss} are the normalised flow and torque losses which may be calculated from the loss model which can take the form of multivariate polynomials

$$q^*_{loss} = \sum_i A_i \left(\frac{|\varpi|}{\varpi_{\max}}\right)^{n_{1,i}} \left(\frac{|\Delta p|}{\Delta p_{\max}}\right)^{n_{2,i}} |x|^{n_{3,i}} \tag{9}$$

$$t^*_{loss} = \sum_i B_i \left(\frac{|\varpi|}{\varpi_{\max}}\right)^{n_{4,i}} \left(\frac{|\Delta p|}{\Delta p_{\max}}\right)^{n_{5,i}} |x|^{n_{6,i}} \tag{10}$$

The set of coefficients A_i, B_i and exponents $n_{1,i}$, $n_{2,i}$, $n_{3,i}$, $n_{4,i}$, $n_{5,i}$, $n_{6,i}$ of the loss model can be calculated from first principles where the particulars of the design are well understood or, more commonly, can be found by curve fitting experimental data. The use of normalised loss terms is an extension of traditional practice and is used to facilitate the selection of the optimum value of D without necessitating the compilation of a new loss model for each alternative size of motor. Caution must be exercised when using this approach because, within any given family of machines, while ΔP_{max} is usually independent of D, the same is not true of ω_{max}, which usually decreases as D increases. The motor performance data used in this paper was taken from [11]. This formulation assumes that the normalised losses are the same in motoring and pumping mode which is not strictly true; with more complete experimental data distinct models could be developed for each mode.

The power lost in the rotating hydraulic machine is:

$$\phi_{loss} = q_{loss}\Delta p + t_{loss}\omega \tag{11}$$

The maximum flow through the pump/motor, neglecting flow losses, is:

$$Q_{\max} = D\omega_{\max} \tag{12}$$

B. Performance of the Hydraulic Cylinder

The assumed characteristics of the cylinder are that the leakage flow is negligible and that the seal friction is low but not quite negligible. This is consistent with current commercial practice in hydraulic cylinder design which is primarily concerned with load holding and prevention of cylinder drift. Future cylinder designs, optimised for wave energy, might allow higher leakage in exchange for extended operating life. The flow generated by the cylinder is:

$$q_{cyl} = vA_{cyl} \tag{13}$$

The frictional forces in the hydraulic cylinder seals are represented by a coulomb damping plus a term proportional to the applied pressure difference.

$$f_{frict} = -\left(D_{bore} + D_{rod}\right)\left(C_0 + C_1\left|\Delta p_{cyl}\right|\right)\operatorname{sign}(v) \tag{14}$$

The structure of equation (14) is as given by [12] and the coefficients, C0 and C1, were calculated from data in [13].
The force actuated by the hydraulic cylinder is

$$f_{pto} = \Delta p_{cyl} A_{cyl} + f_{frict} \tag{15}$$

The power lost in the hydraulic cylinder is

$$\phi_{frict} = f_{frict} v \tag{16}$$

C. Sizing of Pipes, Valves and Cylinder Ports

A rule-based design approach is applied to the sizing of the pipes, valves and cylinder ports. The pipe sizing design parameter, χ, is defined as the ratio of the pumping power loss at maximum flow to the system's maximum fluid power throughput at simultaneous maximum flow and maximum differential pressure, where

$$\chi = \frac{Q_{\max}\,\Delta p_{pipe}\big|^{\max}_{\text{flow}}}{Q_{\max}\Delta P_{rv}} = \frac{\Delta p_{pipe}\big|^{\max}_{\text{flow}}}{\Delta P_{rv}} \tag{17}$$

This means that for any given combination of ΔP_{rv}, Q_{max} and pipe length, the pipe, valve and port sizes can be calculated to

give the required performance. A significant advantage of the approach is that, in the system simulation, the pressure drop can be calculated directly from χ before the pipe lengths or diameters are calculated. This is particularly useful at the early stages of a design investigation because generally the pipe lengths for a particular design depend strongly on the cylinder length and the required cylinder length is not known until after the simulation has run.

The flow is seen to be turbulent so it is reasonable to assume that the pressure drop is proportional to the square of the volumetric flowrate. The pressure drop, Δp_{pipe}, and power loss, ϕ_{pipe}, due to pipe flow in the system are therefore:

$$\Delta p_{pipe} = -\chi \Delta P_{rv} \frac{q\,|q|}{Q_{\max}{}^2} \tag{18}$$

$$\phi_{pipe} = \Delta p_{pipe} q \tag{19}$$

Further research is necessary to determine the economic optimum value and careful checks are necessary to establish technical limits on the feasible values of χ.

V. Model of the Variable Pressure System

The simulation used to assess the variable pressure PTO system is a pseudo-steady-state model. Inherent, in this type of model, is the assumption that the steady-state performance of each item of equipment is representative of its performance in unsteady conditions. It is further assumed that compressibility effects in the hydraulic fluid are negligible; hence there is no mass or volume storage in the system and the instantaneous flows sum to zero. In the variable pressure system neglecting fluid compressibility does not equate to neglecting an energy loss, energy stored elastically in fluid pressurisation is recovered in fluid depressurisation.

A simplification necessary to satisfy the no-storage condition in the type of circuit modelled is to neglect the dynamics associated with changes in the motor displacement fraction. In practice, especially in the case of the swash plate or bent axis axial piston machines, these dynamics can be a significant constraint on the design and a more sophisticated dynamic simulation is needed to further qualify any designs that are given favourable indications by this pseudo-steady-state analysis.

The initial model reported here does not include the electrical machine. A consequence of this limitation on the scope of the model is that the results provided are useful only for operating points where the generator is known to have a high efficiency. In practical terms this means that the current model can provide useful results for high speed synchronous generation but needs some further development before it is capable of providing useful results for variable speed generation. This further work is currently in hand.

The losses considered in the model are:

- Motor conversion losses,
- Cylinder friction losses,
- Pipe flow pumping losses, and
- Relief valve losses.

At cylinder flows up to the maximum motor flow, the flow through the hydraulic motor is equal to the cylinder flow, at cylinder flows above the maximum motor flow the motor flow is fixed at its maximum:

$$q_{mot} = \begin{cases} q_{cyl} & \text{if } |v| \le v_{\lim} \\ Q_{\max} \operatorname{sign}(v) & \text{otherwise} \end{cases} \tag{20}$$

The flow through the relief valve is

$$q_{rv} = \left| q_{cyl} - q_{mot} \right| \tag{21}$$

which evaluates to zero when $|v| \le v_{lim}$. The magnitude in equation (21) represents the rectifying action of the check valves shown around the relief valve in the circuit diagram.

The pressure differential across the motor, ΔP_{mot}, is calculated differently depending on whether the force control has saturated or not. Equation (22) gives ΔP_{mot} in terms of the force command, f_{cmd}, as:

$$\Delta p_{mot} = \begin{cases} \left(\dfrac{f_{cmd} - f_{frict}}{A_{cyl}} - \Delta p_{pipe} \right) & \text{if} \left(|v| \le v_{\lim} \right) \bullet \\ & \left(|f_{cmd}| \le F_{\max} \right) \\ -\Delta P_{rv} \operatorname{sign}(v) - \Delta p_{pipe} & \text{otherwise} \end{cases} \tag{22}$$

where $q=q_{mot}$ is used in evaluating Δp_{pipe} and ϕ_{pipe}. The pressure differential across the piston in the cylinder is:

$$\Delta p_{cyl} = \Delta p_{mot} + \Delta p_{pipe} \tag{23}$$

The power absorbed by the PTO from the ocean is:

$$\phi_{cyl} = f_{PTO} v \tag{24}$$

The shaft power supplied by the motor to the generator is:

$$\phi_{shaft} = \omega t_r \tag{25}$$

Where t_r is the motor torque given by equation (6) above. The power loss through relief valve flow, is:

$$\phi_{rv} = \Delta P_{rv} q_{rv} \tag{26}$$

The time domain simulation was implemented in Simulink®, where, at each time step, the system simulation calculates, in the following sequence, the quantities required to arrive at a simulated PTO force and the minimum set of variables required to facilitate an energy balance in post processing:

1. q_{cyl}, q_{mot}, q_{rv} & Δp_{pipe}
2. Δp_{mot}, Δp_{cyl} & f_{frict}
3. f_{pto} & ϕ_{cyl}

A slight complication is that at step 2 a point iteration is necessary because the cylinder friction depends on the cylinder pressure differential which, for a given force command, cannot be calculated before the frictional force is known. This iteration is implemented in an embedded Matlab function within the Simulink model which eliminates the algebraic loop which would otherwise occur.

As a post processing operation, after the simulation has run, the following additional quantities are calculated:

a. x & q_{loss} (solves for x to satisfy $q_r = q_{mot}$)
b. t_r, ϕ_{shaft}, ϕ_{frict}, ϕ_{pipe}, ϕ_{rv} & ϕ_{loss}

A second point iteration is necessary at step a. in the post processing because it is usually not possible to express x as an

explicit function of q_r. The quantities given by step b. allow an energy balance and an analysis of the system performance.

D. *Performance of the VP PTO System – Steady-State*

The simulation was initially used to determine the steady-state performance of the PTO system. Uncoupled from any WEC device and so from any particular input sea state the performance was calculated for a range of input velocities and force commands. The steady state PTO efficiency is calculated as:

$$\eta_{ss} = \frac{\phi_{shaft}}{\phi_{cyl}} \tag{27}$$

Figure 3 shows the steady state PTO efficiency for a system with a conventional axial piston type motor and Figure 4 shows the same for a system with a Digital Displacement® type motor by Artemis Intelligent Power Ltd. as reported by Payne [7] and Cruz [11]. As discussed in Section V above the efficiency of the downstream mechanical to electrical conversion is not yet included. However, for high speed synchronous generation this additional efficiency is high and so, in its absence, the results are still meaningful.

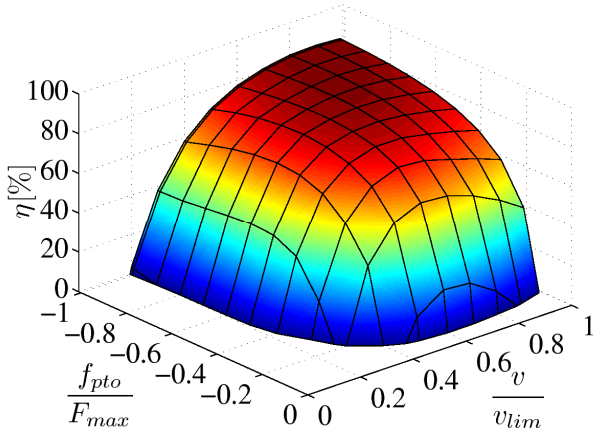

Figure 3 Steady-state performance of a single cylinder single motor Variable Pressure PTO with a conventional axial piston motor running at a constant speed of 1500rpm.

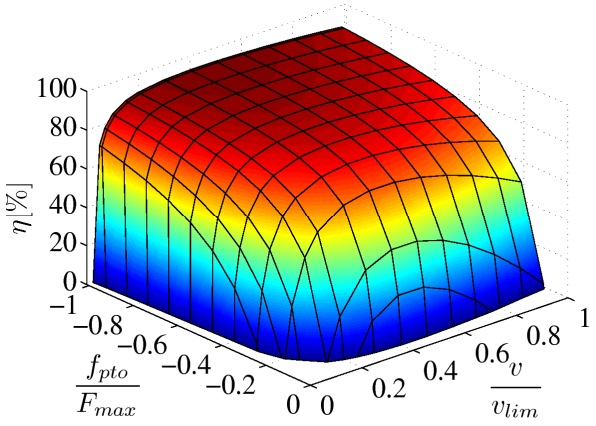

Figure 4 Steady-state performance of a single cylinder single motor Variable Pressure PTO with a Digital Displacement™ motor running at a constant speed of 1500rpm.

The surfaces plotted in Figure 3 and 4 show all operating points with a positive steady-state efficiency. The blank L-shaped region at low velocity and low force is where the power input at the cylinder is less than the power losses in the PTO system. In this region, the steady-state efficiency tends to lose its meaning but in the time domain simulations the power flows at these operating points are integrated and are correctly represented in the energy balance and in the average efficiency for a monochromatic or panchromatic sea state.

The relief valve flow is zero at all of the operating points included in the surfaces above and the cylinder friction is low; therefore, the dominant considerations which determine the performance shown are the pipe flow losses and the motor conversion losses. Of these two the pipe flow losses are identical for each motor type and so it follows that the difference between the two diagrams is due to the superior performance of the Digital Displacement® motor.

There are several measures that can be taken to increase the efficiency of the system with the conventional axial piston motor. Most of these take the form of adaptations to the circuit diagram but the most straightforward is to choose variable, rather than fixed, speed electrical generation. This would allow the motor to operate at closer to its maximum displacement fraction for a greater proportion of the time which would reduce the rate at which the efficiency surface in Figure 3 falls away with decreasing velocity.

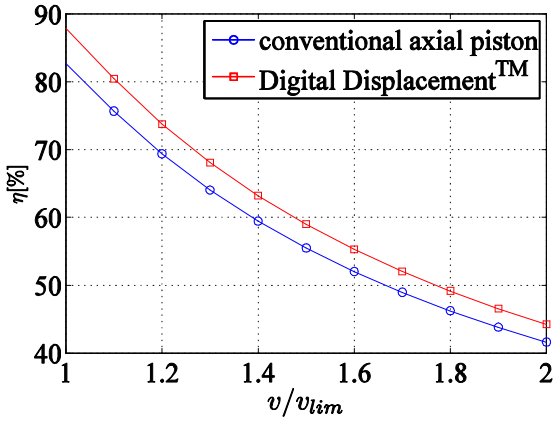

Figure 5 Reduction in efficiency due to relief valve flow at operating points where the $q_{cyl} > Q_{max}$.

For the two motors already discussed Figure 5 shows the reduction in efficiency due to relief valve losses at values of $|v|/v_{lim}>1$. The results are in the form of a single line rather than a surface since only a single force value is possible when $|v|/v_{lim}>1$. The reduction in efficiency indicated is perhaps the strongest reason why the simplest form of the variable pressure PTO system is not a practical proposition. The peak efficiency shown in Figure 3 occurs at $|v|/v_{lim}=1$ and, as a consequence, an optimised system would operate close to this point for as much of the time as possible and inevitably energy would needlessly be lost through relief valve flow. With a relatively simple extension to the circuit the excess flow which passes through the relief valve could be stored in an accumulator and the energy that this flow represents could be converted at close to the system's peak efficiency. Designs such as those presented in [14] and [15] address this problem and also give some additional flexibility and control options.

E. *Performance of Variable Pressure PTO System – Coupled to a WEC*

In order to assess the performance of the PTO in a panchromatic sea state, the PTO model was coupled to a time domain model of a Wavebob. The Wavebob is a large two-body self-reacting axi-symmetric point absorber with the PTO acting in relative heave [16][17]. The time domain model and the geometry used are similar to that described by [17].

In order for the PTO to be effective, a controller which calculates a force set point is necessary. Ideally, the controller would maximise the energy exported from the device. In order to do this, the optimisation of the control parameters must take into consideration both the power absorption from the sea and the power transmission efficiency of the PTO.

For simplicity, we initially limit our investigation to controllers that effect forward power flow only. Reverse power flow from device to sea, as is necessary, for example, in reactive control, is excluded for now. A consequence of this choice is that f_{pto} is constrained to cross zero as v crosses zero. We also initially choose to limit ourselves to a control law where f_{pto} is a function of v only. Taken together, these choices mean that the operating point of the PTO, when represented on force-velocity plane, will start at the origin, (v=0,F=0) and will move from the origin into either of the forward power flow quadrants as the magnitude of the velocity increases and will return to the origin along the same path as the magnitude of the velocity decreases. The restrictions on the control law described are neither a property of the PTO modelled nor are they a necessary property of the controller but a voluntary limitation imposed by the researchers to make the initial investigations more manageable.

We can infer some desirable qualities of the control law by looking at what happens as the operating point meets the limits at F_{max} and v_{lim}. If the path intersects the line f_{pto}=F_{max} at any velocity less than v_{lim} then some energy is wasted through needless relief valve flow. If the path intersects the line at v=v_{lim} at any force other than F_{max}, there will be a discontinuity in f_{pto} (because f_{pto}=F_{max} when v>v_{lim}). Therefore, a desirable behaviour of the controller is that the force set point is always less than F_{max} when v<v_{lim} but equal to F_{max} when v=v_{lim}.

We can infer some further desirable qualities of the control law by looking at the nature of the efficiency surfaces in Figure 3 and Figure 4. Three distinct regions can be identified; firstly, along either the force or velocity axes where no power is absorbed from the sea, secondly, a low force low velocity region, near both axes, where some power is absorbed but little or none is exported due to losses, and thirdly, a high force, high velocity interior where high power is absorbed and is converted at high efficiency. The path that the operating point travels along must traverse the area of low efficiency near the axes before reaching the area of high efficiency in the interior. A good strategy will not absorb, at points of low efficiency, energy that can be stored upstream of the PTO, in both potential and kinetic energy for later absorption into the PTO and conversion at a substantially higher efficiency.

It seems reasonable to speculate that a good control law parameterisation is one that allows the controller to choose the starting point on the *F=0 or v=0* axis to cross through the low efficiency region into the high efficiency region. A piecewise control law with a single parameter that allows this flexibility and satisfies the requirements at the v_{lim} boundary is shown in Figure 6. In response to changes in the measured velocity the force command moves along either the force or velocity axis and at some point leaves the axis and follows a straight line to ($+v_{lim}$,$-F_{max}$) or ($-v_{lim}$,$+F_{max}$).

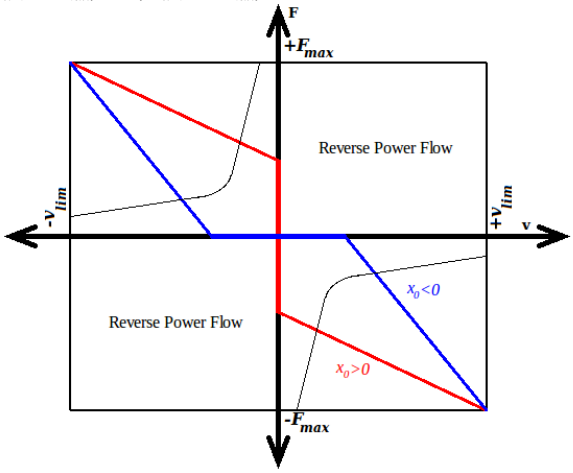

Figure 6 The control law with examples of x_0>0, red, and x_0<0, blue. Only quadrants II and IV, forward power flow, are used. A notional boundary between the low and high efficiency areas is also drawn.

The control law parameter, x_0, indicated in Figure 6, determines which axis is initially followed and how far the operating point moves along the axis before moving into the interior of the F-v plane. The equation of the path that the operating point follows in the interior of the F-v plane is:

$$f_{\text{int}} = F_0 + \frac{|v|}{v_{\text{lim}}}\left(F_{\text{max}} - F_0\right) \tag{28}$$

where F_0 is intercept of the operating point path and the force axis:

$$F_0 = \begin{cases} x_0 F_{\text{max}} & \text{if}\left(x_0 \geq 0\right) \\ \dfrac{x_0}{1+x_0} F_{\text{max}} & \text{if}\left(x_0 < 0\right) \end{cases} \tag{29}$$

The control law used to calculate the force command in the coupled hydraulic hydrodynamic simulation is:

$$f_{cmd} = \begin{cases} -\text{sign}(v) f_{\text{int}}\left(1 - e^{-|v|/v_{ref}}\right) & \text{if}\left(x_0 > 0\right) \\ -\text{sign}(v) f_{\text{int}} & \text{if}\left(x_0 \leq 0\right)\left(f_{\text{int}} > 0\right) \\ 0 & otherwise \end{cases} \tag{30}$$

The exponential component in equation (30) is added to avoid a force discontinuity at v=0 when x_0>0 and v_{ref} is chosen to be sufficiently small so that this filtering component does not significantly affect the power flows.

The surface plots in Figure 7 to Figure 9 show selected power flows in the system for the optimal x_0 value at each combination of A_{cyl} and D. The other necessary input parameters were held constant at:

$$\varpi = 1500\frac{2\pi}{60}\frac{\text{rad}}{\text{s}}, \qquad \Delta P_{rv}=40\text{MPa}, \qquad \chi=8\%$$

The sea state used was H_s=4.5m and T_e=8.75s which is close to the highest probability sea state in the Belmullet scatter diagram by Mollison [18]. The average powers are calculated by averaging the relevant instantaneous power over the repeat period of the sea state in a portion of the simulation after the initial transients have died away.

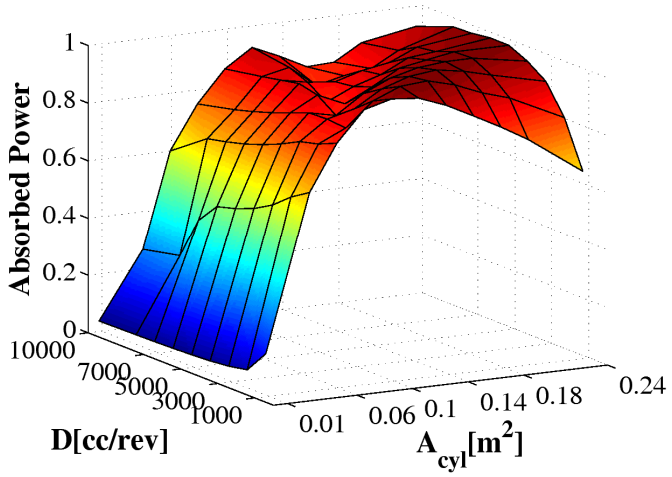

Figure 7 Normalised average absorbed power for a Variable Pressure PTO system with a conventional axial piston motor.

Figure 7 and Figure 8 show, respectively, the primary power absorbed from the sea and the secondary shaft power transmitted to the generator by the device with a Variable Pressure PTO using a conventional axial piston motor. The power levels indicated are of the order of several hundred kilowatts but because the exact power levels are commercially sensitive the values are normalised with respect to the highest absorbed power. For the sea state and the control law used the highest absorbed power is 8% higher than the maximum with optimised linear damping in the same simulation.

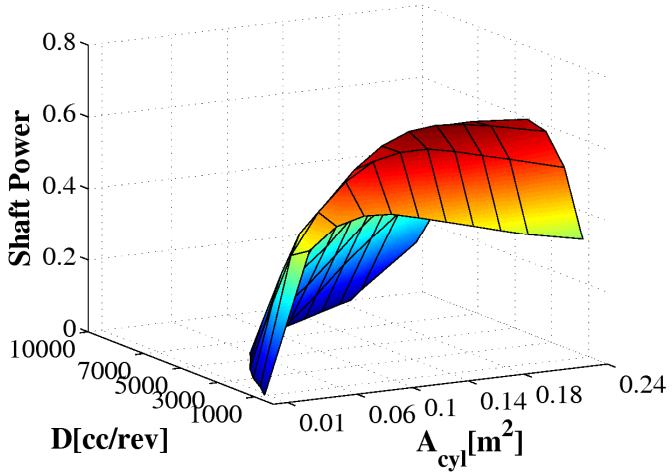

Figure 8 Normalised average shaft power for Variable Pressure PTO system with a conventional axial piston motor.

Two local maxima in absorbed power are evident; this is probably an artefact of the simplified, and overly restrictive, control law parameterisation. The area between the two local maxima corresponds to combinations of D and A_{cyl} where the optimal value of x_0 is close to 0. It is hoped that by adding only one or two more points to the piecewise control law this valley could be removed and a slightly improved maximum revealed.

A single local maximum is evident in the shaft power surface. Away from the local maximum, the reduction in power is due to: increasing motor losses at higher D and lower A_{cyl} values, increasing pipe flow losses at higher A_{cyl} values, and increasing relief valve losses at lower D values.

Figure 9 shows the shaft power for a variable pressure PTO in the same device and the same sea state but with a Digital Displacement® motor. The power is again normalised with respect to the highest absorbed power, which is almost identical for both motors. The peak shaft power, however, is higher in Figure 9 than in Figure 8 and, in Figure 9, there is a wide area where the performance is almost as high as the peak. The performance at larger motor displacements is vastly superior to that of the axial piston motor.

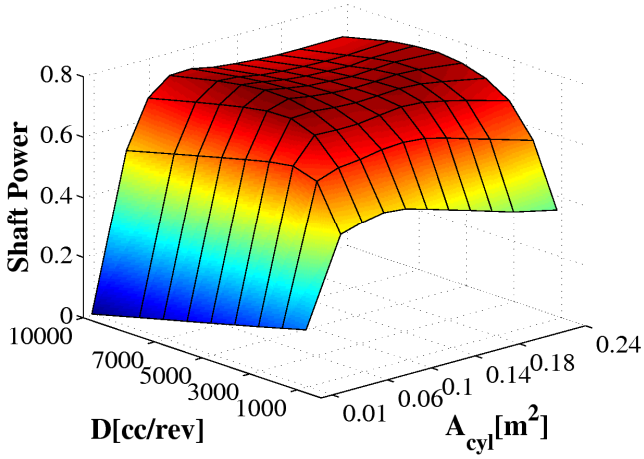

Figure 9 Normalised average shaft power for Variable Pressure PTO system with a Digital Displacement® motor.

The sizes of the equipment indicated are large, by any standards. It should be noted that the optimal D values are about 4 to 10 times those of the machines which yielded the loss models underlying the calculation.

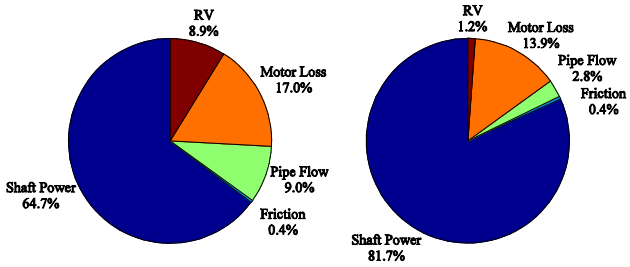

Figure 10 Comparison of power flows in best examples of variable pressure PTO system. Conventional axial piston (left) and Digital Displacement® (right) motors. Fixed speed 1500RPM in both cases.

Comparing the values of D and A_{cyl} that give the highest power values in Figure 8 and in Figure 9 reveals that the peak for the Digital Displacement® motor occurs at about twice the value of D and half the value of A_{cyl} as it does for the conventional axial piston motor. Figure 10 gives a comparison between the power flows in the systems represented by the highest shaft power values in Figure 8 and Figure 9. This analysis reveals a complexity not apparent from the steady state

efficiency surfaces. The improvement in shaft power comes about through:

- A decrease in the relief valve flow which results from the larger motor and smaller cylinder.
- A reduction in the pipe flow losses since, for equal values of χ, the power lost to pipe flow is proportional to $(vA_{cyl})^3/D^2$.
- A reduction in the power lost in the motor due to the inherent advantages of the Digital Displacement® motor.

Of the auxiliary systems not yet included in the analysis, parasitic power consumption due to the charge pump and the cooling system are also likely to be less in the case of the PTO with the Digital Displacement® motor than in the case of the conventional axial piston motor because the motor flow loss and overall heat dissipation are both reduced. The parasitic power consumption due to filtration is more difficult to anticipate.

The results presented are for a single panchromatic sea state, while work to extend this to a scatter diagram, representative of a whole year, is in hand. An important component of the task of the designer of these systems is to choose values of the hardware parameters, D and A_{cyl}, so that the WEC controller can be effective in all sea states that are likely to contribute significant energy during the typical year. The shaft power delivered by the Digital Displacement® motor is remarkably insensitive to the choice of these hardware parameters and so the prospects for high efficiency over a full year are probably good. The shaft power delivered by the conventional axial piston motor is somewhat more sensitive to the hardware parameters, but, as discussed above, this could be improved by choosing variable speed generation.

VI. Model of a Constant Pressure PTO System

The model of the constant pressure system used is also a pseudo steady state model. The steady state performance of the equipment is again assumed to be representative of its performance in unsteady conditions. The principal additional assumption relates to the accumulators: It is assumed that the accumulators are sufficiently large that their pressure remains constant irrespective of flow accumulation, so that ΔP_{rv} also specifies the pressure difference between the accumulators.

The flow pumped from low to high pressure, q_{pmp}, due to the combination of cylinder and directional control valve is

$$q_{pmp} = q_{cyl} x_v \tag{31}$$

where $x_v \in \{-1,0,1\}$ is the position of the directional control valve. To apply the most basic usage of the constant pressure circuit, the control law for the directional control valve is

$$x_v = \text{sign}(v) \tag{32}$$

In this simulation the motor flowrate q_{mot} is

$$q_{mot} = \begin{cases} 0 & \text{if } \left(\bar{q}_{pmp} \le 0\right) \\ -\bar{q}_{pmp} & \text{if } \left(0 < \bar{q}_{pmp} < Q_{\max}\right) \\ -Q_{\max} & \text{otherwise} \end{cases} \tag{33}$$

where $\bar{q}_{pmp}$ is the time average of q_{pmp} over the entire simulation. In a more realistic model, with pressure variations in the accumulators and particularly where there is an economic selection of accumulator volume, q_{mot} must be dynamically controlled as a compromise between accumulator pressure control and power smoothing.

The rate of flow to the high pressure (and therefore from the low pressure accumulator), q_{acc}, is

$$q_{acc} = q_{pmp} + q_{mot} \tag{34}$$

Because the assumptions allow for truly constant accumulator pressure the relief valve is almost completely redundant and q_{rv} will evaluate to zero for all combinations where $|q_{mot}|$ is less than Q_{max}

$$q_{rv} = \begin{cases} 0 & \text{if } (\bar{q}_{pmp} < 0) \\ \bar{q}_{pmp} + q_{mot} & \text{otherwise} \end{cases} \tag{35}$$

Also, due to constant accumulator pressures, the motor pressure differential is fixed

$$\Delta p_{mot} = \Delta p_{rv} \tag{36}$$

The cylinder pressure differential is

$$\Delta p_{cyl} = -\Delta p_{rv} x_v + \Delta p_{pipe} \tag{37}$$

where $q=q_{cyl}$ is used in evaluating Δp_{pipe} and ϕ_{pipe}. An assumption in equation (37) is that the flow related pressure loss is independent of the valve position, and so is independent of whether the cylinder is loaded or idle. This is a simplification but is reasonable in a preliminary investigation since the pipes on the cylinder side of the valve are likely to be longer than the pipes on the motor side and the valve itself is likely to account for a significant proportion of the flow resistance.

Special attention must be paid to the periods in the simulation where the relative velocity between the two bodies is zero and the relative excitation force is not high enough to initiate relative motion against the PTO. In a PTO that allows reverse flow this mode does not occur, because the PTO force, rather than the excitation force, initiates the motion. In a passive constant pressure PTO, where the excitation force provides the cylinder pressurisation the relative velocity will be fixed at zero until the cylinder pressure rises to the accumulator pressure and flow between the cylinder and the accumulator, and so motion of the device is possible. Equation (38) gives a reasonable approximation to the behaviour of the PTO force as the device passes through this pressurisation phase:

$$f_{pto} = A_{cyl} \Delta p_{cyl} \left(1 - e^{-|v|/v_{ref}}\right) \tag{38}$$

With an appropriate choice of v_{ref} the exponential rise causes the pressurisation to occur at very low velocities rather than strictly at zero velocity. A check calculation confirms that the energy absorbed at pressures less than 99.5% of ΔP_{cyl} is negligible.

The fluid is again assumed to be incompressible; the justification for this is more nuanced in the case of the constant pressure system than it is in that of the variable pressure system. If the valve control law is anything other than passive rectification then valve opening events would cause depressurisation of a volume of fluid and loss of the elastic energy stored in that volume. As noted in [6], a high frequency of these events would reduce system efficiency considerably and so this effect, where it occurs, should be quantified. In the case of passive rectification however the cylinder valves can

only open when the pressure difference across them is zero and so the stored elastic energy is never lost.

The time domain simulation was implemented in Simulink® where, similarly to the variable pressure simulation, the following quantities are calculated, in the following sequence, at each time step:

1. q_{cyl}, x_v, q_{pmp}, q_{mot}, q_{acc}, q_{rv} & Δp_{pipe}
2. Δp_{mot}, Δp_{cyl} & f_{frict}
3. f_{pto} & ϕ_{cyl}

As a post processing operation, after the simulation has run, the following quantities are calculated to allow an energy balance.

a. x & q_{loss} (solves for x to satisfy q_r=q_{mot})

b. t_r, ϕ_{shaft}, ϕ_{frict}, ϕ_{pipe}, ϕ_{rv} & ϕ_{loss}

Point iterations are again required at step 2 and at step a.

F. *Performance of a Constant Pressure System – Coupled to a WEC*

To assess the performance of the PTO in a panchromatic sea state, the PTO model was coupled to a time domain model of a Wavebob. The model and geometry are similar to that described by [17]. The sea state used was H_s=4.5m and T_e=8.75s which is close to the highest probability sea state in the Belmullet scatter diagram [18].

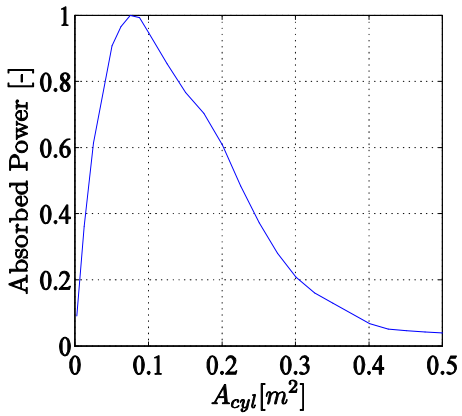

Figure 11 Normalised average absorbed power for a constant pressure PTO with passive rectification.

The volumetric flows at the primary and secondary sides of the constant pressure PTO are decoupled. Under the assumptions made, this decoupling is complete and the motor selection or operation does not affect the absorbed power, which is a function of the PTO force, the control law and the choice of the piping design parameter. For passive rectification and given relief valve pressure set point the power absorbed is a function of the chosen A_{cyl} and this relationship is plotted in Figure 11.

The shaft power output from the PTO to the generator is shown for a constant pressure PTO with a conventional axial piston motor in Figure 12 and a Digital Displacement® motor in Figure 13. In each case, the power is normalised with respect to the highest absorbed power in Figure 11.

Both Figure 12 and Figure 13 show a single local maximum in power output from the PTO for the chosen sea state. Away from the optimum A_{cyl}, the shaft power falls due to reduced absorbed power. At lower than optimum D values, the relief valve losses start to become significant and at higher than optimum D values the motor losses become more significant because of increased operation at lower displacement fractions. This last effect is much more significant in the case of the conventional axial piston motor than in the case of the Digital Displacement® motor.

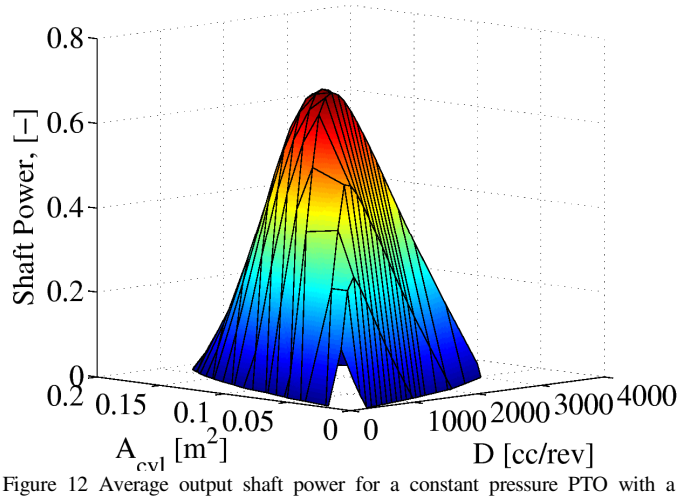

Figure 12 Average output shaft power for a constant pressure PTO with a conventional axial piston motor running at constant 1500RPM.

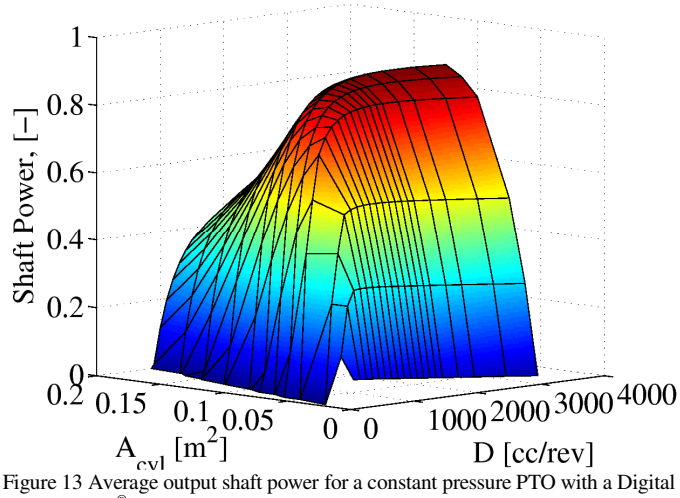

Figure 13 Average output shaft power for a constant pressure PTO with a Digital Displacement® motor running at constant 1500RPM.

The sizes of equipment indicated in Figure 12 and Figure 13 for the constant pressure PTO are smaller than those in Figure 8 and Figure 9 for the variable pressure PTO. The peak power in Figure 12 occurs at a motor displacement that is just within the range that is commercially available at present.

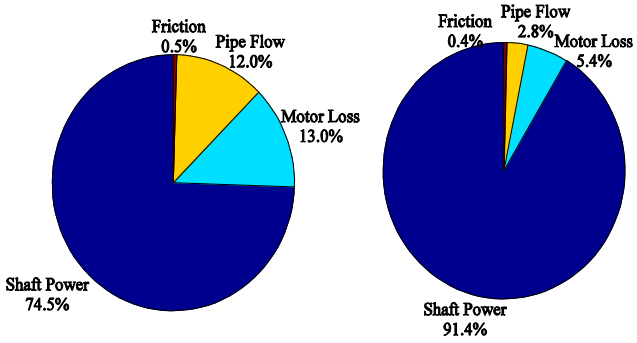

Figure 14 Comparison of power flows in best examples of constant pressure PTO system. For conventional axial piston (left), Digital Displacement® (right) motors. Fixed speed 1500RPM in both cases.

Figure 14 gives a comparison of the power flows in the systems represented by the highest powers in Figure 12 and Figure 13. The values of A_{cyl} and D at these points are such that the average cylinder flow is less than the maximum motor flow, which means that losses due to relief valve flow do not feature in Figure 14.

VII. CONCLUSIONS

Table 1 gives a summary of results for each combination of the variable pressure and constant pressure systems considered with the conventional axial piston motor on one hand and the more recently developed Digital Displacement® motor on the other. The absorbed and shaft powers are normalised with respect to the highest absorbed power from the entire investigation.

TABLE 1 SUMMARY OF RESULTS

System:	Variable Pressure PTO		Constant Pressure PTO	
Motor Type:	Axial piston	Digital Displacement®	Axial piston	Digital Displacement®
Highest Absorbed Power:	100%	100%	96%	96%
Highest Shaft Power:	65%	78%	69%	88%
PTO efficiency:	65%	81%	74%	91%

The conclusions which may be drawn from the analysis are:

- Of the combinations of system concept and motor technology presented above, notwithstanding the spread in efficiencies, all possibilities are worthy of further investigation and development.
- The sensitivities of the shaft power to the design parameters are such that the difference between the conventional motor and the Digital Displacement® motor is likely to increase when a wider range of input sea states is considered.
- The efficiency of the variable pressure system would benefit from the addition of integrated accumulator storage to that system.

These results must be viewed as preliminary because:

- The results are calculated for a single short term sea-state rather than for a complete year.
- Only fixed speed generation is considered.
- The assumptions made in the analysis are suitable for a preliminary assessment but would not be satisfactory for design finalisation.

Further work to extend the investigation to the full Belmullet scatter diagram of Mollison [18] and to include the electrical generation in the model is in hand. It is hoped that this completed analysis will help to make clear whether and what adaptations of the basic circuits are advantageous.

Adaptations which might improve PTO efficiency or increase flexibility so that PTO efficiency can be maintained over a wider range of input conditions include: Addition of accumulator storage to the variable pressure circuit; additional cylinders, motors or generators in either circuit; utilisation of variable speed generators in either circuit. Finally, more advanced control, tailored to each type of PTO system, is necessary.

The most important increments which might be made in the modelling approach are, firstly inclusion of accumulator gas processes, secondly of swash plate dynamics in the axial piston motor and thirdly of fluid de-pressurisation losses where control of the constant pressure circuit involves valve transitions at points other than the velocity zero crossing. Quantification of auxiliary power consumed by the charge pump and case flushing is also necessary.

ACKNOWLEDGMENT

The financial support of Enterprise Ireland, project number IP/2009/0024, is gratefully acknowledged.

REFERENCES

[1] B.M. Count, "The theoretical analysis of wave power devices with non-linear mechanical conditioning" CEGB Laboratory Note 1008, 1978.

[2] A. Falcao, "Modelling and control of oscillating-body wave energy converters with hydraulic power take-off and gas accumulator" Ocean engineering, vol. 34, pp2021-2032, 2007.

[3] A. Babarit, M. Guglielmi, and A.H. Clément, "Declutching control of a wave energy converter" Ocean Engineering, vol. 36, pp1015-1024, 2009.

[4] F. Fusco, and J.V. Ringwood, "Suboptimal Causal Reactive Control of Wave Energy Converters Using a Second Order System Model" Proceedings of the 21st International Offshore (Ocean) and Polar Engineering Conference (ISOPE), Maui, USA, 2011.

[5] G. Bacelli, J.V. Ringwood, and J,-C. Gilloteaux, "Control of a wave energy device for potable water production" Proc. European Control Conf., pp 3755-3760, 2009.

[6] R. Henderson, "Design, simulation, and testing of a novel hydraulic power take-off system for the Pelamis wave energy converter" Renewable energy, vol. 31, pp271-283, 2006.

[7] G.S. Payne, U.B.P. Stein, M. Ehsan, N.J. Caldwell, and W.H.S. Rampen, "Potential of digital displacement hydraulics for wave energy conversion" Proceedings of the Sixth European Wave and Tidal Energy Conference, Glasgow, 2005.

[8] A.R. Plummer and M. Schlotter "Investigating the Performance of a Hydraulic Power Take-Off", Proceedings of the Eight European Wave and Tidal Energy Conference, Uppsala, 2009.

[9] R. Yemm, "Pelamis WEC – Full-Scale Joint System Test", Report to DTI, V/06/00191/00/00/REP, DTI URN 03/1435, 2003.

[10] J. Ivantysyn, and M. Ivantysynova, *Hydrostatic pumps and motors: principles, design, performance, modelling, analysis, control and testing*, 1st English ed. Tech Books International, 2003.

[11] J. Cruz, *Ocean Wave Energy*, Springer, 2008.

[12] H.K. Müller, and B.S. Nau, *Fluid Sealing Technology*, Marcel Dekker, 1998.

[13] B. Ederle, "New Hydraulic Sealing Systems. Requirements and Trends", 8th Bath fluid power conference, paper D3, pp337-259, 1998.

[14] S.H. Salter, J.R.M. Taylor, and N.J. Caldwell, "Power conversion mechanisms for wave energy" Proc. IMechE, Part M, vol 216, pp1-27, 2002.

[15] K. Schlemmer, F. Fuchsumer, N. Böemer, R. Costello, and C. Villegas, "Design and control of a Hydraulic Power Take Off in an Axi-symmetric Heaving Point Absorber", Proceedings of the Nineth European Wave and Tidal Energy Conference, Southampton, 2011.

[16] W. Dick, "Wave Energy Converter," U.S. Patent 7 581 901, Sept. 1, 2009.

[17] J.J. Candido, and P.A.P. Justino, "Frequency, Stochastic and Time Domain Models for an Articulated Wave Power Device", Proc. ASME 27th OMAE, Portugal, 2008.

[18] D. Mollison, "Ireland's wave power resource: a report to the NTSB and the ESB", Dublin, 1982.